American Mineralogist, Volume 89, pages 1610–1616, 2004

Nanometer-scale measurements of $Fe^{3+}/\Sigma Fe$ by electron energy-loss spectroscopy: A cautionary note

LAURENCE A. J. GARVIE,[1,*] THOMAS J. ZEGA,[1,†] PETER REZ,[3] AND PETER R. BUSECK[1,2]

[1]Department of Geological Sciences, Arizona State University, Tempe, Arizona 85287-1404, U.S.A.
[2]Department of Chemistry and Biochemistry, Arizona State University, Tempe, Arizona 85287-1604, U.S.A.
[3]Department of Physics and Astronomy, Arizona State University, Arizona 85287-1504, U.S.A.

ABSTRACT

The effects of electron-beam damage on the $Fe^{3+}/\Sigma Fe$ (total iron) ratio were measured by electron energy-loss spectroscopy (EELS) with a transmission electron microscope (TEM). Spectra were acquired from crushed and ion-beam-thinned cronstedtite. For fluences below 1×10^4 e/Å^2, the $Fe^{3+}/\Sigma Fe$ values from crushed grains range between 0.43 and 0.49, consistent with undamaged material. These measurements were acquired from flakes 180 to 1000 Å thick. With increase in fluence, samples <400 Å thick become damaged and exhibit $Fe^{3+}/\Sigma Fe$ values >0.5. The critical fluence for radiation damage by 100 kV electrons as defined by $Fe^{3+}/\Sigma Fe$ <0.5 for cronstedtite at 300 K, is 1×10^4 e/Å^2. The absorbed dose to the speciman during acquisition of a typical EELS spectrum is large, with values around 2.2×10^{10} Gy (J/kg), equivalent to the deposition of 620 eV/Å^3. Cooling to liquid N_2 temperature did not significantly slow the damage process. Ion-beam thinning produces an amorphous layer on crystal surfaces. Spectra from the thinnest regions, which are amorphous, exhibit $Fe^{3+}/\Sigma Fe$ >0.7. With increase in sample thickness, the $Fe^{3+}/\Sigma Fe$ values decrease to a minimum, consistent with data from the undamaged material. The increase of $Fe^{3+}/\Sigma Fe$ with respect to electron-beam irradiation is likely caused by loss of H. At low fluences, the loss of H is negligible, thus allowing consistent $Fe^{3+}/\Sigma Fe$ values to be measured. The cronstedtite study illustrates the care required when using EELS to measure $Fe^{3+}/\Sigma Fe$ values. Similar damage effects occur for a range of high-valence and mixed-oxidation state metals in minerals. EELS is the only spectroscopic method that can be used routinely to determine mixed-valence ratios at the nanometer scale, but care is required when measuring these data. Consideration needs to be given to the incident beam current, fluence, fluence rate, and sample thickness.

INTRODUCTION

Electron energy-loss spectroscopy (EELS) with a transmission electron microscope (TEM) is a powerful method for determining oxidation state at the nanometer scale (Sauer et al. 1993; Garvie et al. 1994; Garvie and Craven 1994; Garvie and Buseck 1998, 1999; van Aken and Liebscher 2002). EELS spectra of different monovalent Fe-bearing minerals exhibit distinct $L_{2,3}$ edge shapes and chemical shifts, whereas minerals containing Fe^{2+} and Fe^{3+} exhibit L_3 edges that are intermediate in shape between the two single-valence end-members (Garvie and Buseck 1998; van Aken and Liebscher 2002). The changes in relative heights of the L_3 edge maxima reflect changes in $Fe^{3+}/\Sigma Fe$ (Garvie and Buseck 1998; van Aken and Liebscher 2002; Zega et al. 2003).

Accurate determination of $Fe^{3+}/\Sigma Fe$ requires spectra free of damage induced by the electron beam. Damage effects observed in inorganic materials in the TEM include hole drilling (Duscher et al. 1998), element loss (Champness and Devenish 1992), sample decomposition and formation of new materials (Rez et al. 1995; Zenser and Gruehn 2001), change in coordination of elements (van Aken et al. 1998), and change in oxidation state (Garvie and Craven 1994; Garvie and Buseck 1999). Beam damage is usually accompanied by amorphization of the sample (e.g., van Aken et al. 1998), although new materials can form under the beam. For example, electron irradiation under high electron fluences causes thorianite (ThO_2) to react with the C film of the TEM grid to form a Th carbide. Also, $Be(OH)_2$, LiF, and $FeCl_2 \cdot nH_2O$ can decompose to the metal (Garvie, unpublished data).

The effect of the electron beam on inorganic materials depends on factors that include incident electron energy, probe-current density, dimensions of the irradiated volume, and sample temperature (Egerton et al. 1987; Inui et al. 1990; Champness and Devenish 1992). In addition, the structure of the material and presence of water and OH will affect the rate and type of damage caused by the beam. Studies of ionic inorganic solids have shown that the primary damage effect is decomposition, for example, transformation of $CaCO_3$ to CaO. This damage results from the effects of ionization within the irradiated area by the incident electron beam (Hobbs 1979). At high fluence rates it is also possible to remove cations such as Al^{3+} in minerals (Champness and Devenish 1992).

Certain metals are susceptible to reduction in the TEM by the

* E-mail: lgarvie@asu.edu
† Current address: Naval Research Laboratory, Code 6360, 4555 Overlook Ave. SW, Washington, D.C. 20375, U.S.A.

electron beam. For example, high-valence metals such as Mn^{7+} and Mn^{4+} are reduced to Mn^{2+} (Garvie and Craven 1994) and Ce^{4+} to Ce^{3+} (Garvie and Buseck 1999). The opposite change also occurs where the metal oxidation state increases as a result of beam damage, for example, in H-bearing minerals, and may be related to H loss (Garvie et al. 1994).

The goals of this paper are to illustrate the electron-beam susceptibility of minerals containing Fe^{3+} and Fe^{2+} using cronstedtite $(Fe^{2+}_{3-x}Fe^{3+}_{x})[Si_{2-x}Fe^{3+}_{x}O_5](OH)_4$, where $0 < x < 1$ (Hybler et al. 2000) as an example, and to compare the effects of sample preparation on the quality of the acquired data. Cronstedtite was chosen because it is relatively stable to beam damage and contains abundant $Fe^{2+}$and Fe^{3+}. These characteristics allow the beam damage to be studied in real time and good spectra to be acquired with short acquisition times.

Materials and methods

Cronstedtite from Kisbanya, Romania and the Cold Bokkeveld CM chondrite meteorite was studied. A single jet-black crystal from Kisbanya was crushed gently in methanol, and a small drop of the fine mineral in suspension was dried on a Cu TEM grid coated with lacey amorphous C. The Cold Bokkeveld sample was prepared by mounting a Cu ring onto the area of interest on a petrographic thin section (Zega and Buseck 2003). The ring with the sample was removed from the thin section and thinned to electron transparency using a Gatan precision ion-polishing system (PIPS). The PIPS was operated at a constant 3 rpm rotation rate, acceleration voltages of 2.5 to 5.0 keV, and Ar-ion bombardment angles of 2.5 to 6.0°. Initial thinning was done at higher keV and angles to mill the bulk of the material.

Spectra were acquired at room and liquid-N_2 temperatures with a GATAN 766 DigiPEELS spectrometer attached to a Philips 400-ST field-emission-gun (FEG) TEM. The TEM was operated at an accelerating voltage of 100 kV, with probe currents that ranged from 0.3 to 4.0 nA. The current on the sample was measured with a Faraday cup placed in front of the beam in the microscope and was recorded with a picoammeter. The width at half maximum, and hence the energy resolution, of the zero-loss peak was 0.8 eV. Spectra were acquired in diffraction mode (the spectrometer is image coupled), which allowed control of the collection angle, 2β. Typical values for the beam-convergence semi-angle, α, and collection semi-angle, β, were 16 and 11 mrad, respectively.

The beam-damage literature uses a confusing and often nonstandard nomenclature for terms such as fluence and fluence rate. In addition, fluence and fluence rate can be expressed in several alternate units, making comparisons with the literature problematic. For clarity, the terminology and units used in this study are described in the Appendix.

We define three incident current ranges: low (<0.8 nA), medium (0.8 to 1.8 nA), and high (>1.8 nA). The divisions between these ranges are arbitrary, and the terms low, medium, and high are structure and element dependent. Hence, the numerical values of the ranges are specific to cronstedtite. Dividing the probe current by the irradiated area of the sample per second gives the fluence rate, which is the number of electrons incident per unit area per second. A typical fluence rate was 2×10^3 e/(Å^2·s).

Spectra were acquired with acquisition times of 2 to 8 seconds. Because of the incomplete readout characteristics of the Gatan DigiPEELS, the first spectrum of a pair was not saved. For example, an 8 s spectrum was saved every 16 seconds. Hence, we distinguish between acquisition and irradiation times. Specimen thicknesses were greater than $0.1 \times \lambda_T$, where λ_T is the inelastic mean-free path (Egerton 1996). Using the procedures in Egerton (1996, p. 305), we estimated λ_T to be 900 Å (see Appendix), which is accurate to within 15% (Crozier 1990), giving calculated specimen thicknesses of 100 to 1760 Å. Spectra were acquired from areas 50 to 600 nm in diameter.

A background of the form AE^{-r} was subtracted from the core-loss edges, and the effects of the tailing of the zero-loss peak were deconvoluted using a point-spread-function spectrum. Details of spectrum acquisition and processing are given in Garvie and Buseck (1999). Spectra for the damage studies were acquired using the "Acquire to disk" feature of the Gatan el/p program, which allows multiple spectra to be acquired from a single point, with a set acquisition time per spectrum. For this study, we chose a 4 s acquisition time as this interval allows spectra with good signal to be acquired for the quantification.

The $Fe^{3+}/\Sigma Fe$ values were determined using the shapes of the Fe L_3 edge, with a multiple, linear, least-squares fitting routine with Fe^{3+} and Fe^{2+} spectra as end-members (Garvie and Buseck 1998; Zega et al. 2003). The mixed-valence spectra exhibit characteristics of the two end-member, single-valence spectra. They were simulated by linear combinations of fayalite (Fe_2SiO_4) as the model Fe^{2+} end-member, and a composite spectrum of hematite, aegirine, and synthetic leucite, with $^{IV}Fe^{3+}$ representing the Fe^{3+} end-member (Zega et al. 2003). The composite spectrum permitted optimal fitting because it accommodated variations in the fine structure that arise from differences in coordination and bonding. The Fe^{3+} and Fe^{2+} L_3 reference spectra were scaled to each other by normalizing their edges to the continuum above the edge onset. In this way, the integrated areas of the L_3 edges are quantifiably related and reflect the oxidation state of the Fe.

Results and discussion

The Fe $L_{2,3}$ edges from terrestrial and meteoritic cronstedtites free of electron-beam damage are shown in Figure 1, together with the end-member fitting spectra. The fayalite and hematite-aegirine-leucite L_3 peak maxima are at 707.8 and 709.5 eV, respectively. The Fe L_3 edge maximum of cronstedtite exhibits a two-peaked edge that is intermediate in shape between the two single-valence end-members, with peak energies that are similar to their single-valence end-members. Quantification of $Fe^{3+}/\Sigma Fe$ for the Cold Bokkeveld cronstedtite reveals ratios of 0.48 to 0.54, consistent with previous measurements (Zega et al. 2003). The Kisbanya cronstedtite exhibits $Fe^{3+}/\Sigma Fe$ between 0.43 and 0.49. Eighteen spectra acquired from one large, uniformly thick flake gives an $Fe^{3+}/\Sigma Fe$ value of 0.45, with a standard deviation of ±0.02. There were marked differences in the quality of data that were acquired from thin areas of crushed vs. ion-beam-thinned cronstedtite, and these two sample types are discussed below.

Crushed cronstedtite

The $Fe^{3+}/\Sigma Fe$ values for 10 flakes under low-current conditions, i.e., <0.8 nA, show values of 0.43 to 0.46, consistent with undamaged material. These spectra were acquired with fluence

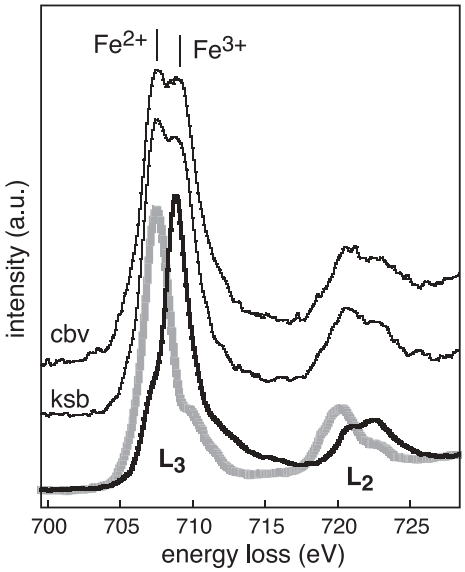

Figure 1. Representative Fe $L_{2,3}$ edges of cronstedtite from Kisbanya (ksb) and the Cold Bokkeveld (cbv) CM chondrite, compared with spectra from fayalite (Fe^{2+}) and the composite hematite/aegirine/leucite (Fe^{3+}) spectrum. For clarity, the fayalite spectrum is gray and the hematite/aegirine/leucite spectrum is bold.

rates of between 100 and 600 e/(Å^2·s), for sample thicknesses between 400 and 900 Å. Under these experimental conditions, the $Fe^{3+}/\Sigma Fe$ values are independent of the incident current, thickness, fluence rate, and fluence, and show conditions under which spectra are acquired free of measurable electron-beam damage effects. These fluence rates are high compared with those required for examination of organic and biological materials in the TEM, where damage typically occurs for rates >10 e/(Å^2·s) for 100 kV electrons (Ciliax et al. 1993; Ohno et al. 2002).

Ratios measured from 40 flakes range from 0.43 to 0.69 for incident currents of 0.3 to 4.0 nA (Table 1). Changes in the $Fe^{3+}/\Sigma Fe$ values depend on the electron fluence rate and sample thickness (Fig. 2). For fluence rates below 800 e/(Å^2·s), the $Fe^{3+}/\Sigma Fe$ values measured from crushed material range between 0.43 and 0.47, consistent with undamaged material. These measurements were acquired from flakes 180 Å to 1000 Å thick. Flakes <500 Å thick became damaged at fluence rates above 800 e/(Å^2·s), as revealed by higher values of $Fe^{3+}/\Sigma Fe$.

To explore the effects of high electron fluences on $Fe^{3+}/\Sigma Fe$, series of spectra were acquired with the electron beam stationary on a small region of sample. These series, acquired at room and liquid-N_2 temperature, allowed the ratio change to be monitored as a function of time and hence electron fluence. Ten spectra were acquired from each region with a 4 s acquisition time. During irradiation, the shape of the Fe L_3 edge changes markedly, $Fe^{3+}/\Sigma Fe$ increases (Fig. 3), and the irradiated area amorphises.

Areas thinner than 400 Å show higher $Fe^{3+}/\Sigma Fe$ values than the undamaged material after the first eight seconds of irradiation (Fig. 4). Thicker areas produce $Fe^{3+}/\Sigma Fe$ values between 0.44 and 0.48, consistent with undamaged material. With continued irradiation and therefore increase in fluence, all areas show an increase in $Fe^{3+}/\Sigma Fe$ values. In general, thinner samples damage more rapidly than thicker ones. The damage series for the room temperature and cooled samples behave similarly, with an increase in $Fe^{3+}/\Sigma Fe$ with respect to fluence. The cooled samples are only moderately more beam stable than the room temperature ones. In contrast, cooling fluorinated organics to liquid-nitrogen temperatures can reduce F loss by several orders of magnitude (Ciliax et al. 1993).

The plot of thickness against fluence for undamaged ($Fe^{3+}/\Sigma Fe$

TABLE 1. Representative data for $Fe^{3+}/\Sigma Fe$, thickness, fluence rate, and fluence for Kisbanya cronstedtite

$Fe^{3+}/\Sigma Fe$	Thickness (Å)	Fluence rate e/(Å^2 s)	Fluence (e/Å^2)
0.43	830	550	3300
0.43	1450	3100	25000
0.43	440	330	200
0.43	660	130	1100
0.44	1070	3200	2600
0.44	500	100	800
0.45	1150	3410	27000
0.45	720	540	4300
0.45	660	3300	26000
0.45	910	500	3000
0.46	370	130	1100
0.46	900	3600	29000
0.47	580	3500	28000
0.51	300	3000	24000
0.53	410	3200	26000
0.56	200	2500	20000
0.56	230	2800	22000
0.63	150	3000	24000
0.69	110	2400	19000

Note: Error for $Fe^{3+}/\Sigma Fe$ is ±0.02, for thickness is ±7%, for fluence rate and fluence is ±20%.

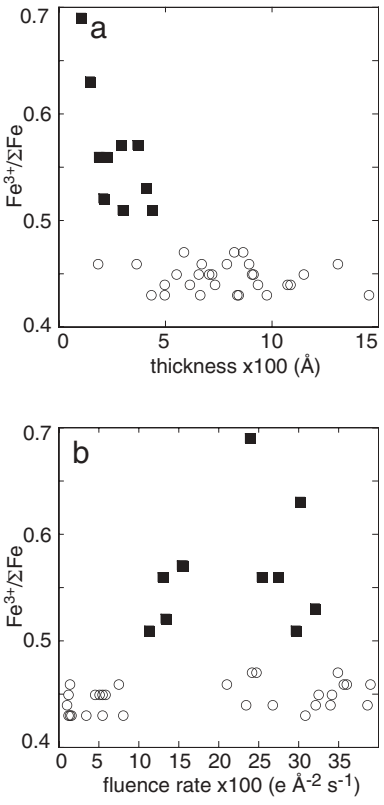

FIGURE 2. $Fe^{3+}/\Sigma Fe$ values measured from Kisbanya cronstedtite for 40 crystals plotted against (**a**) thickness and (**b**) fluence rate. Incident current ranged from 0.3 to 4.4 nA. The solid squares represent damaged cronstedtite and open circles undamaged cronstedtite. Error for $Fe^{3+}/\Sigma Fe$ is ±0.02, thickness is ±7%, and for fluence rate is ±20%.

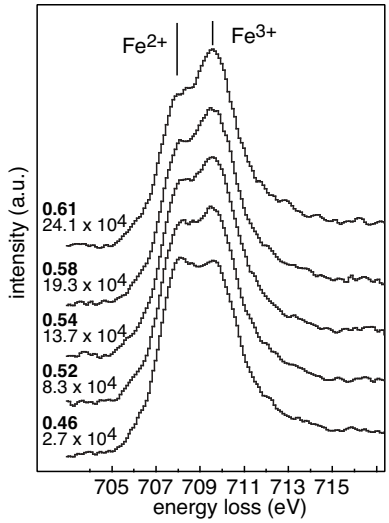

FIGURE 3. Fe L_3 edge of the Kisbanya cronstedtite from one grain illustrated as a function of fluence. The measured $Fe^{3+}/\Sigma Fe$ value (bold) and fluence (e/Å^2) are indicated above each spectrum.

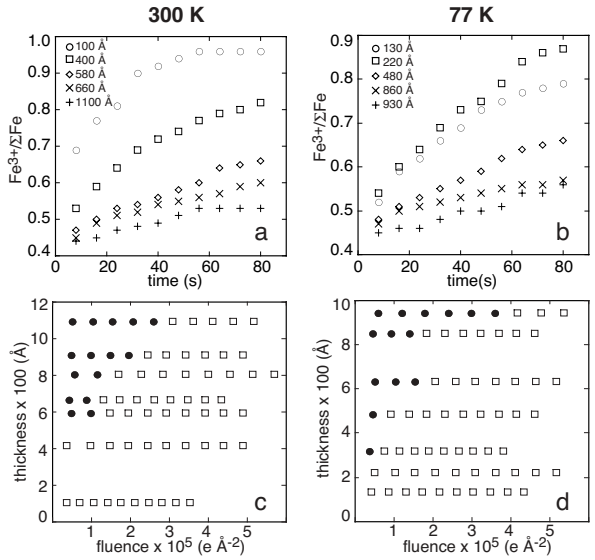

FIGURE 4. $Fe^{3+}/\Sigma Fe$ values measured from Kisbanya cronstedtite at room (300 K) and liquid N_2 temperature (77 K) for different thicknesses. The effect of thickness and fluence are evident from plots (**c**) and (**d**). Spectra with $Fe^{3+}/\Sigma Fe > 0.5$ are indicated by the open squares and undamaged data by filled circles. Spectra were acquired with fluence rates of 1000 e/(Å^2·s). Error for $Fe^{3+}/\Sigma Fe$ is ±0.02, thicknesses are accurate to ±7%, and fluence to ±20%.

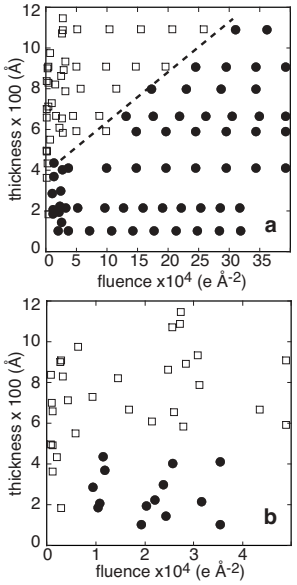

FIGURE 5. Plots of thickness against fluence. Filled circles are for $Fe^{3+}/\Sigma Fe$ values >0.5 and represent damaged material. Open squares represent undamaged material. **(a)** The dotted line separates the damaged from undamaged material. **(b)** The low fluence plot allows the critical fluence, f_c, to be measured.

<0.5) and damaged ($Fe^{3+}/\Sigma Fe$ >0.5) cronstedtite exhibits three distinct regions (Fig. 5). Below a fluence of 1×10^4 e/Å^2, all values of $Fe^{3+}/\Sigma Fe$ are <0.5. Between fluences of 1×10^4 and 5×10^4 e/Å^2, the boundary between damaged and undamaged data (Fig. 5b) is horizontal with a critical thickness of 500 Å separating these data. At higher fluences, $>5 \times 10^4$ e/Å^2, the boundary between the damaged and undamaged data is separated by a positive linear slope. The critical fluence, f_c, is measured from the plot of thickness against fluence (Fig. 5). This fluence is the value below which the $Fe^{3+}/\Sigma Fe$ values remain constant. For our experiments, $f_c = 1 \times 10^4$ e/Å^2. The complexity of the boundary between the damaged and undamaged data as a function of thickness against fluence (Fig. 5) suggests a range of competing processes involved in the damage. Below the critical fluence, the rate of damage is lower than the rate of healing events (Champness and Devenish 1992).

The O:Fe ratio remains constant over five orders of magnitude of fluence as determined from the O *K* and Fe $L_{2,3}$ edges (Fig. 6a). In addition, the sample thickness also remains constant for similar fluences (Fig. 6b). These results indicate that loss of O is not the cause of the changes in $Fe^{3+}/\Sigma Fe$ with respect to increase in fluence, and that sample sputtering from the irradiated regions is negligible. The increase of $Fe^{3+}/\Sigma Fe$ with respect to electron-beam damage is likely caused by loss of H from the irradiated areas as H is mobile under the electron beam. The lack of a major temperature dependence of the damage rate suggests that H diffusion is not significant. It is still possible that the activation energy for diffusion is sufficiently low that there might not be an observed decrease with temperature. One would expect that diffusion would be more significant in thinner specimens and hence the damage would decrease with thickness.

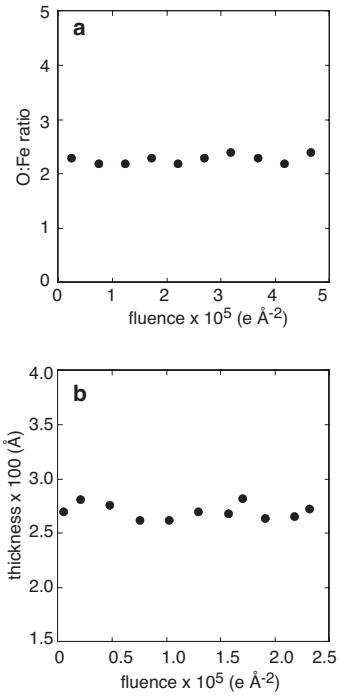

FIGURE 6. Plots of (**a**) O:Fe ratio and (**b**) thickness against fluence for one grain of Kisbanya cronstedtite.

There is a similar increase in $Fe^{3+}/\Sigma Fe$ after heating cronstedtite to ca. 300 °C, which Mackenzie and Berezowski (1981) attributed to the loss of hydroxyl water. A log plot of the fractional loss of Fe^{2+} against fluence reveals linear relationships (Fig. 7) and hence an exponential rate of change in $Fe^{3+}/\Sigma Fe$.

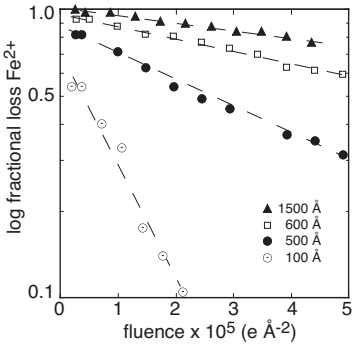

FIGURE 7. A plot of log fractional loss of Fe^{2+} against fluence for four different sample thicknesses. Error for fluence is ±20%.

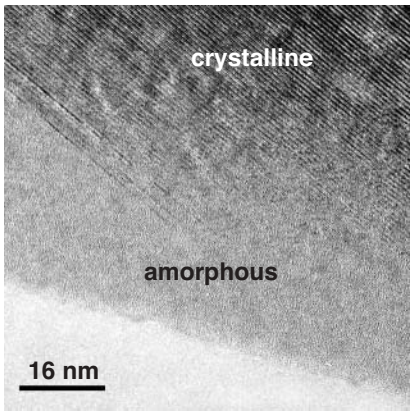

FIGURE 8. HRTEM image of ion-beam-thinned cronstedtite from the Cold Bokkeveld chondrite. Note the wide amorphous edge.

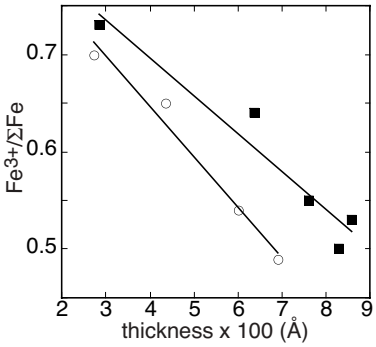

FIGURE 9. A plot of $Fe^{3+}/\Sigma Fe$ values vs. sample thickness for two wedge-shaped, ion-beam-thinned crystals (open and closed symbols) of Cold Bokkeveld cronstedtite. Error for $Fe^{3+}/\Sigma Fe$ is ±0.02 and thicknesses are accurate to ±7%.

TABLE 2. $Fe^{3+}/\Sigma Fe$ and thickness for two ion-beam-thinned cronstedtite crystals from Cold Bokkeveld

$Fe^{3+}/\Sigma Fe$	Thickness (Å)
Crystal 1	
0.70	270
0.65	440
0.54	600
0.49	690
Crystal 2	
0.73	280
0.64	640
0.55	760
0.50	830
0.53	860

Note: Error in $Fe^{3+}/\Sigma Fe$ is ±0.02 and thickness is ±7%.

Ion-beam-thinned cronstedtite

Sample preparation by ion-beam thinning has the advantage of producing large electron-transparent areas for TEM analysis. This method is especially useful for fine-grained heterogeneous materials such as rims and matrix of carbonaceous chondrites (e.g., Zega and Buseck 2003). Unfortunately, ion milling causes surface damage that can alter the characteristics of the material. Surface amorphization is ubiquitous, and the thickness of this layer depends on factors such as the incident ion angle and accelerating voltage (Barber 1993; Barna et al. 1999; McCaffrey et al. 2001).

Samples of the Cold Bokkeveld chondrite prepared by ion-beam thinning reveal lath-shaped cronstedtite crystals with large areas suitable for EELS measurements. The ion-thinned samples clearly reveal an amorphous edge (Fig. 8). Quantification of 44 areas with thicknesses of 700 Å or greater show $Fe^{3+}/\Sigma Fe$ values of 0.48 to 0.54 (Zega et al. 2003). Ratios from thinner areas are higher.

Series of spectra were acquired from progressively thicker areas of two grains of ion-beam-thinned cronstedtite, i.e., from the thin amorphous edge to a thickness of 850 Å, with a fluence rate around 3000 e/(Å^2·s) (Table 2). The spectra from the amorphous edge, which was 300 Å thick, had $Fe^{3+}/\Sigma Fe$ >0.7 (Fig. 9). With an increase in sample thickness, the $Fe^{3+}/\Sigma Fe$ data decreased to values consistent with the undamaged sample, revealing the importance of acquiring spectra from relatively thick areas. For the acquisition conditions used here, crystal thicknesses of >700 Å were needed to measure consistent $Fe^{3+}/\Sigma Fe$ values from samples that were ion-beam thinned. In contrast, under similar fluences, correct $Fe^{3+}/\Sigma Fe$ values could be obtained from crushed cronstedtite with a thickness of >280 Å.

Therefore, caution is required when acquiring data from ion-beam-thinned samples for Fe and other metals that can occur in different oxidation states. Thinning produces an oxidized surface layer, and so spectra must be acquired from thicknesses where the signals from the undamaged material dominate those from the amorphous surfaces.

Energy deposited by the electron beam

The energy available for radiation damage can be estimated from the electron energy-loss spectrum (see Appendix) (Rez and Glaisher 1991). The total energy deposited in the specimen per incident electron $E_D = \int P(E) \times E \, dE$, where $P(E)$ is the probability of an electron losing energy E. E_D has units of eV.

Determination of E_D for four spectra, with $t/\lambda < 1$, reveals values between 12 and 47 eV (Fig. 10a, Table 3). These values are an upper limit as a small fraction of the deposited energy is removed by processes such as X-ray emission and secondary electrons (Rez and Glaisher 1991). Plotting E_D against thickness reveals a linear relationship, with the values tending toward 0 eV for zero thickness. For the cronstedtite, a plot of E_D against thickness gives $E_D = 0.06t$, where thickness is in angstroms.

The absorbed doses for these experiments are large, ranging

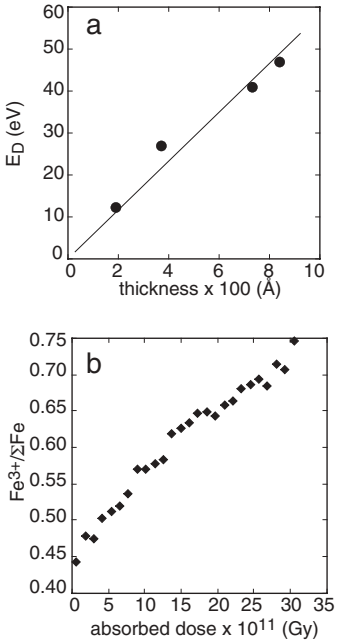

FIGURE 10. (**a**) Comparison of energy deposited per incident electron, E_D, against thickness. (**b**) Representative damage series plotted as a function of absorbed dose.

TABLE 3. Energy deposited per incident electron, E_D, and absorbed dose for four cronstedtite spectra

Sample	Thickness (Å)	Radius (Å)	Fluence (e/Å^2)	E_D (eV)	Absorbed dose $\times 10^{10}$ (Gy)
Ksbrt34	190	1300	10344	12	2.2
Ksbrt26	370	1300	44152	27	3.3
Ksbrt29	730	1030	9360	41	2.5
Ksbrt37	840	4200	880	47	0.24

Notes: All samples have a t/λ <1.

from 2.4×10^9 to 3×10^{12} Gy (Fig. 10b). Absorbed dose is measured in the SI unit of gray (Gy), which has dimensions of J/kg. The magnitude of the absorbed doses is the reason for electron-beam damage in the TEM. For comparison, typical electron doses for electrons in human radiation therapy are <100 Gy, and $<5 \times 10^4$ Gy is used for electron-beam sterilization (Kotov et al. 2003). From the absorbed doses we can estimate the energy deposited per unit volume, which is typically around 600 eV/Å^3.

Acquiring $Fe^{3+}/\Sigma Fe$ values free of damage effects

We observed damage effects similar to those in cronstedtite in all minerals with Fe^{2+} and Fe^{3+} that contain structural H. Similar oxidation changes were noted for other 3d transition elements (Garvie et al. 1994). Our studies of hydrous Fe-bearing minerals reveal a range of susceptibilities to changes in oxidation state. For example, using samples of similar thickness, Fe-rich biotite was damaged with fluences of >50 e/Å^2 as compared to cronstedtite, which damaged for fluences of >5000 e/Å^2. Although the current study concentrates on oxidation of Fe under moderate fluence rates, it is also possible to reduce high-valence metals (Garvie and Craven 1994; Garvie and Buseck 1999).

The amount of Fe in the sample will dictate the quality of data that can be acquired and thus the accuracy of the measured ratios. Low Fe concentrations require longer EELS acquisition times, with a concomitant increase in fluence and thus an increased possibility of electron-beam damage. In summary, although EELS is the only spectroscopic method that can be used routinely to determine mixed-valence ratios at the nanometer scale, care is required when measuring these ratios. Consideration needs to be given to the incident beam current, fluence, fluence rate, and sample thickness, although the $Fe^{3+}/\Sigma Fe$ values are often independent of thickness below a critical fluence.

ACKNOWLEDGMENTS

We thank two anonymous reviewers for their helpful suggestions and comments. This work was funded by grants from the National Science foundation (NSF EAR 00-87714, 01-13345, DMR 99-72670) and NASA (NAG5-9352).

REFERENCES CITED

Barber, D.J. (1993) Radiation damage ion-milled specimens: characteristics, effects and methods of damage limitation. Ultramicroscopy, 52, 101–125.
Barna, Á., Pécz, B., and Menyhard, M. (1999) TEM sample preparation by ion milling/amorphization. Micron, 30, 267–276.
Champness, P.E. and Devenish, R.W. (1992) Radiation damage in silicate minerals: implications of AEM. In A. López-Galindo and M.I. Rodríguez-García, Eds., Electron Microscopy 92, vol. II: Materials Sciences, p. 541–545. Secretariado de Publicaciones de la Universidad de Granada, Granada, Spain.
Ciliax, B.J., Kirk, K.L., and Leapman, R.D. (1993) Radiation damage of fluorinated organic compounds measured by parallel electron energy loss spectroscopy. Ultramicroscopy, 48, 13–25.
Crozier, P.A. (1990) Measurement of inelastic electron scattering cross-sections by electron energy-loss spectroscopy. Philosophical Magazine, 61, 311–336.
Duscher, G., Browning, N.D., and Pennycook, S.J. (1998) Atomic column resolved electron energy-loss spectroscopy. Physica Status Solidi A, 166, 327–342.
Egerton, R.F. (1996) Electron Energy-Loss Spectroscopy in the Electron Microscope. (Second Edition) Plenum Press, New York.
Egerton, R.F., Crozier, P.A., and Rice, P. (1987) Electron energy-loss spectroscopy and chemical change. Ultramicroscopy, 23, 305–312.
Garvie, L.A.J. and Buseck, P.R. (1998) Ferrous/ferric ratios from nanometer-sized areas in minerals. Nature, 396, 667–670.
——— (1999) Electron-beam induced solid-state reduction of Ce(IV) to Ce(III) in cerianite (CeO_2) studied by electron energy-loss spectroscopy (EELS). Journal of Physics and Chemistry of Minerals, 60, 1943–1947.
Garvie, L.A.J. and Craven, A.J. (1994) Electron-beam-induced reduction of Mn^{4+} in manganese oxides as revealed by parallel EELS. Ultramicroscopy, 54, 83–92.
Garvie, L.A.J., Craven, A.J., and Brydson, R. (1994) Use of electron-loss near-edge fine structure in the study of minerals. American Mineralogist, 79, 411–425.
Hobbs, L.W. (1979) Radiation damage in electron microscopy of inorganic solids. Ultramicroscopy, 3, 381–386.
Hybler, J., Petříček, V., Ďurovič, S., and Smrčok, L. (2000) Refinement of the crystal structure of cronstedtite-1*T*. Clays and Clay Minerals, 48, 331–338.
Inui, H., Mori, H., Sakata, T., and Fujita, H. (1990) Electron irradiation induced crystalline-to-amorphous transition in quartz single crystals. Journal of Non-Crystalline Solids, 116, 1–15.
Kotov, Y.A., Sokovnin, S.Y., and Balezin, M.E. (2003) A review of possible applications of nanosecond electron beams for sterilization in industrial poultry farming. Trends in Food Science and Technology, 14, 4–8.
Mackenzie, K.J.D. and Berezowski, R.M. (1981) Thermal and Mossbauer studies of iron-containing hydrous silicates. III. Cronstedtite. Thermochimica Acta, 44, 171–187.
McCaffrey, J.P., Phaneuf, M.W., and Madsen, L.D. (2001) Surface damage formation during ion-beam thinning of samples for transmission electron microscopy. Ultramicroscopy, 87, 97–104.
Sauer, H., Brydson, R., Rowley, P.N., Engel, W., and Thomas, J.M. (1993) Determination of coordinations and coordination-specific site occupancies by electron energy-loss spectroscopy: an investigation of boron-oxygen compounds. Ultramicroscopy, 49, 198–209.
Rez, P. and Glaisher, R.W. (1991) Measurement of energy deposition in transmission electron microscopy. Ultramicroscopy, 35, 65–69.
Rez, P., Weiss, J.K., Medlin, D.L., and Howitt, D.G. (1995) Direct measurements of the radiolytic transformation of thin films of titanium dioxide using EELS. Microscopy, Microanalysis, and Microstructures, 6, 433–440.
van Aken, P.A. and Liebscher, B. (2002) Quantification of ferrous/ferric ratios in minerals: new evaluation schemes of Fe $L_{2,3}$ electron energy-loss near-edge spectra. Physics and Chemistry of Minerals, 29, 188–200.
van Aken, P.A., Sharp, T.G., and Seifert, F. (1998) Electron-beam induced amorphization of stishovite: silicon-coordination change observed using Si

K-edge extended electron energy-loss fine structure. Physics and Chemistry of Minerals, 25, 83–93.
Zega, T.J. and Buseck, P.R. (2003) Fine-grained rim mineralogy of the Cold Bokkeveld CM chondrite. Geochimica et Cosmochimica Acta, 67, 1711–1721.
Zega, T.J., Garvie, L.A.J., and Buseck, P.R. (2003) Nanometer-scale measurements of iron oxidation states of cronstedtite from primitive meteorites. American Mineralogist, 88, 1169–1172.
Zenser, L.P. and Gruehn, R. (2001) Decomposition of MgF_2 in the transmission electron microscope. Journal of Solid State Chemistry, 157, 30–39.

MANUSCRIPT RECEIVED OCTOBER 10, 2003
MANUSCRIPT ACCEPTED MAY 25, 2004
MANUSCRIPT HANDLED BY DARBY DYAR

APPENDIX

We use sample ksbrt26 to illustrate the calculations of fluence, fluence rate, energy deposited per incident electron, and absorbed dose. Data were acquired with 1.3 nA of current incident on the sample, 8 s irradiation time, sample thickness of 370 Å, and irradiation radius of 1300 Å.

Determining electron fluence rate and fluence

The terms dose rate and dose are frequently used in TEM-based beam-damage studies. However, the SI terms are electron fluence rate and fluence, which have dimensions of $m^{-2}s^{-1}$ and m^{-2}. Because of the small areas probed in the electron microscope, we use units of electrons per $Å^2$ and per ($Å^2$·s) for fluence and fluence rate, respectively.

For ksbrt26, the current incident on the sample was 1.3 nA, which is equivalent to 7.8×10^9 e/s (since 1nA ≈ 6×10^9 e/s). This also can be quoted as 1.3×10^{-9} A and 1.3×10^{-9} C/s, since 1A = 1 C/s. This current leads to a fluence rate, sometimes called current density or dose rate, of 1.5×10^3 e/($Å^2$·s) (or 1.5×10^5 e/nm^2·s). In the literature, fluence rate is often quoted in A/m^2 and A/cm^2. The fluence rate of 1.5×10^3 e/($Å^2$·s) is equivalent to 2.4×10^4 A/m^2 and 2.4 A/cm^2 (using 1A = 6×10^{18} e/s).

The fluence to the sample is thus the fluence rate multiplied by the spectrum acquisition time.

Determining E_D

Determination of the total energy deposited in the specimen per incident electron is necessary to calculate the energy deposited to the specimen during spectral acquisition. The probability, $P(E)$, of an electron losing energy, E, is given by the normalized energy-loss spectrum:

$$P(E) = I(E)/I_T,$$

where $I(E)$ is the spectral intensity, I, at energy E, and I_T is the total counts in the energy-loss spectrum. The normalized spectrum is just the EELS spectrum with each data point divided by the total spectrum counts. The total energy deposited in the specimen per incident electron, E_D is

$$E_D = \int_{E_{min}}^{E_{max}} P(E) \times E \, dE$$

In practice, this integral can be evaluated as

$$E_D = \Sigma P_j(E_j) \times E_j \times \Delta E,$$

where $P_j(E_j)$ is the normalized probability at energy E_j. The energy interval ΔE is the energy dispersion of the EELS spectrum. E_D has units of eV.

This measure of energy deposited is valid even if there is multiple scattering. The energy deposited will only be linear with thickness when the thickness is less than the inelastic mean free path. At greater thicknesses multiple scattering terms will make contributions that vary with higher powers of thickness.

Determining E_D for several spectra with different thicknesses, for which $t/\lambda < 1$, provides an empirical relationship between E_D and thickness. For the cronstedtite, a plot of E_D against thickness gives $E_D = 0.06\,t$, where t is thickness in angstroms and E_D is in eV.

Determining energy deposited per incident electron

The energy deposited in the sample by the incident electron beam depends on E_D, current incident on the sample, and the dimensions of the irradiated volume. A total of 6.24×10^{10} electrons entered sample ksbrt26, given a current of 1.3 nA and 8 s acquisition time. The empirical relationship between E_D and thickness provided E_D = 22 eV, which is the average energy deposited in the specimen per incident electron, for a thickness of 370 Å.

The energy deposited to the sample is the number of electrons incident on the sample multiplied by E_D. For ksbrt26 this gives 1.4×10^{12} eV, equivalent to 2.2×10^{-7} J (because 1eV = 1.6×10^{-19} J).

Calculating the absorbed dose

Absorbed dose is measured in the SI unit of gray (Gy), which has dimensions of J/kg.

The volume irradiated in ksbrt26 was equal to $\pi \times (1300 \times 10^{-8})^2 \times 370 \times 10^{-8}$, or 2×10^{-15} cm^3. Given a density for cronstedtite of 3.34 g/cm^3, the irradiated volume has a mass of 6.7×10^{-18} kg. Therefore, the absorbed dose is $2.2 \times 10^{-7}/6.7 \times 10^{-18}$, which is equal to 3.3×10^{10} Gy.

Estimation of the inelastic mean-free path λ

From Egerton (1996), p. 305, the mean-free path can be estimated from the relationship:

$$\lambda = \frac{106F(E_0 / E_m)}{\ln(2\beta E_0 / E_m)}$$

where λ is given in nm, β is the collection semiangle in mrad, E_0 is the incident energy in kV, and E_m is the mean energy loss in eV. E_m depends on the composition of the specimen. F is a relativistic factor that is 0.768 for E_0 of 100 kV. E_0 was estimated using $E_m \approx 7.6Z^{0.36}$, where Z is the atomic number. For compounds, Z can be calculated as an effective atomic number Z_{eff} as:

$$Z_{eff} = \frac{\Sigma_i f_i Z_i^{1.3}}{\Sigma_i f_i Z_i^{0.3}}$$

where f_i is the atomic fraction of each element of atomic number Z_i. For cronstedtite, assuming an ideal formula of $Fe_3(SiFe)O_5(OH)_4$, we have

$$Z_{eff} = \frac{22.2 \times 26^{1.3} + 5.6 \times 14^{1.3} + 50.0 \times 8^{1.3} + 22.2 \times 1^{1.3}}{22.2 \times 26^{0.3} + 5.6 \times 14^{0.3} + 50.0 \times 8^{0.3} + 22.2 \times 1^{0.3}} = 13.0$$

for which E_m = 19.2 and λ = 900 Å.